General Disclaimer

One or more of the Following Statements may affect this Document

- This document has been reproduced from the best copy furnished by the organizational source. It is being released in the interest of making available as much information as possible.

- This document may contain data, which exceeds the sheet parameters. It was furnished in this condition by the organizational source and is the best copy available.

- This document may contain tone-on-tone or color graphs, charts and/or pictures, which have been reproduced in black and white.

- This document is paginated as submitted by the original source.

- Portions of this document are not fully legible due to the historical nature of some of the material. However, it is the best reproduction available from the original submission.

X-732-70-344
PREPRINT

NASA TM X- 65353

STABILITY OF SAS-A DUAL SPIN SPACECRAFT WITH ENERGY DISSIPATION ON THE MOMENTUM WHEEL

PETER M. BAINUM

SEPTEMBER 1970

GSFC
GODDARD SPACE FLIGHT CENTER
GREENBELT, MARYLAND

X-732-70-344
PREPRINT

STABILITY OF SAS-A DUAL SPIN SPACECRAFT WITH ENERGY DISSIPATION ON THE MOMENTUM WHEEL

Peter M. Bainum

September 1970

GODDARD SPACE FLIGHT CENTER
Greenbelt, Maryland

ACKNOWLEDGMENT

The research reported here was conducted at the NASA Goddard Space Flight Center, Stabilization and Control Branch where the author was participating as a Faculty Fellow in the NASA-ASEE 1970 Summer Faculty Fellowship Program. My research colleague was Dr. Joseph V. Fedor of the Stabilization and Control Branch whose continued interest and encouragement is greatly acknowledged. In addition, the author would like to express his appreciation to Dr. T. W. Flatley of the Stabilization and Control Branch and Dr. A. K. Sen, Postdoctoral Research Associate in the Stabilization and Control Branch for the many illuminating discussions.

STABILITY OF SAS-A DUAL SPIN SPACECRAFT WITH ENERGY DISSIPATION ON THE MOMENTUM WHEEL

Peter M. Bainum

ABSTRACT

The attitude stability of the SAS-A satellite with damping in the momentum wheel as well as the "despun" portion is analyzed. Wheel energy dissipation is modeled by assuming the wheel can flex with two degrees of freedom relative to the hub. The nonlinear attitude equations are derived for small wheel flexural motion and are a ninth order nonautonomous set. If the main body damper mass and wheel transverse moment of inertia are assumed small when compared with main satellite masses and inertias, an averaging process can be used to determine the zeroth and first order secular perturbations on the behavior of the system nutation angle. From this a general analytic stability criterion is established. A numerical evaluation of this criterion using SAS-A parameters and measured wheel damping data indicates that stability about a zero degree nutation angle is insured by a factor of 128 under normal operating conditions.

CONTENTS

ILLUSTRATIONS

NOMENCLATURE

A, B, C = main body moments of inertia about the x, y, z axes respectively

$\bar{A}, \bar{B}, \bar{C}$ = composite moments of inertia about the x, y, z axes respectively

$\bar{b}_i$ = unit vectors along the x, y, z axes respectively ($i = 1, 2, 3$)

$\bar{b}_i'$ = unit vectors fixed to the nominal plane of the undeflected wheel and rotating with it

C_i = coefficients occurring in the steady state solutions for ϕ_1, α_z, α_x

d_1, d_2 = the inner and outer radius of the rotor rim, respectively

H = magnitude of system angular momentum vector $\bar{H}$

h = thickness of rotor disc

I_{b_i} = moment of inertia of main body about the $\bar{b}_i$ axis

I_{R_i} = moment of inertia of rotor about its b_i axis

I_{d_i} = moment of inertia of the pendulous damper about the $\bar{b}_i$ axis

K = the restoring spring constant of the torsion wire support

K_R = the restoring spring constant of the rotor

$\bar{K} = K/mr_1^2\Omega^2$, dimensionless form of K

k = the nutation damping (rate) constant

k_R = rotor damping constant

ℓ = height of damper plane above x, z plane

L_i = the applied external torques about the $\bar{b}_i$ axis

M = the mass of the main satellite and the rotor

$\bar{M}$ = the total system mass

m = the pendulum end mass

m_R = the mass of the rotor

$q = \bar{B}/\bar{A}$

$q' = I_{R_2}/\bar{A}$

r = radial coordinate of a differential mass on the rotor

r_0 = the distance from the nominal spin (y) axis to the pendulum hinge point

r_1 = the length of the pendulum

s = spin rate of rotor relative to main body

s_{crit} = critical value of s when only one stable equilibrium angle exists

T = kinetic energy

t = time

V = potential energy

x, y, z = principal axes of main satellite

y_R = displacement coordinate of dm_R from plane of undeflected rotor disc

α_z, α_x = rotor deflection angles about the $\bar{b}_3'$, $\bar{b}_1'$ axes respectively

$\Gamma = \ell m/\bar{M}$

γ = the nutation angle, i.e. the angle between the $\bar{b}_2$ axis and $\bar{H}$

$\lambda = \left[(B - A)\Omega + I_{R_2} s\right]/A$, in the zeroth order solution, frequency with which transverse angular velocity component rotate about $\bar{b}_2$ axis

Ω = nominal main body spin rate

ω = in the zeroth order solution, the value of ω_3 at some reference time

ω_i = angular velocities about the x, y, z axes respectively (i = 1, 2, 3)

ϕ = position angle of the projection of dm_R on the plane of the undeflected rotor disc

ϕ_i = nutation damper displacement angle

ρ = density of rotor disc

τ = time constant associated with nutation angle decay

Superscript

( )′ refers to component in b_i' axes system

( )˙ indicates differentiation with respect to time

Subscript

ave refers to averaged quantity

b_i, i refers to particular main body axes (i = 1, 2, 3)

0 refers to initial state or equilibrium value

STABILITY OF SAS-A DUAL SPIN SPACECRAFT WITH ENERGY DISSIPATION ON THE MOMENTUM WHEEL

I. INTRODUCTION

NASA Goddard Space Flight Center is currently directing the design and development of a dual-spin Small Astronomy Satellite (SAS-A) to be launched in the Fall 1970. The satellite will have the capability of scanning the entire celestial sphere to determine the relative position of X-ray emitting sources with respect to the fixed position of the stars. It is important that the attitude of the satellite be precisely known and maintained in order to accurately determine the location of the X-ray emitting sources.

The damping and attitude stability of the SAS-A satellite with damping only on the slowly spinning main part was reported previously.[1] The resulting differential equations of rotational motion when linearized were an autonomous set of fifth order equations with constant coefficients. Analytical stability criteria were developed from these equations using the method of Routh-Hurwitz.

Subsequent to the previous analysis, it has been demonstrated by static and dynamic tests of the SAS-A momentum wheel that there was some energy dissipation in the shaft-momentum wheel assembly. The purpose of the present investigation is to incorporate the effects of momentum wheel damping into the rotational equations of motion for the SAS-A spacecraft, and to analytically investigate the attitude stability of such a system. A possible way to model the wheel energy dissipation is to add a spring-mass-dashpot damper to the wheel similar to the model of Mingori.[2] It is then necessary to relate the dissipation of the dashpot damper to that of the shaft-momentum wheel assembly. Another approach is that used by Sen[3] and Fleisher[3] in which the wheel is assumed to flex with two degrees of freedom with respect to the hub. This latter alternative was selected as a more appropriate model since the results of the momentum wheel tests could be directly used in determining appropriate wheel restoring and damping coefficients.

The present analysis is based upon the dual spin attitude control system consisting of a slowly rotating main part to which is attached the X-ray sensors, a high speed momentum wheel (rotor) whose spin axis is nominally parallel to the main body spin axis, and a pendulous type nutation damper attached to the main part and constrained to move in a plane which is perpendicular to the main body nominal spin axis.

II. ANALYSIS

The satellite, wheel, and damping systems are illustrated in Figure 1. The elements of the attitude control system are: 1) the main part of the spacecraft, essentially a right circular cylinder where the nominal spin axis is the $\bar{b}_2$ body axis, 2) a small momentum wheel or rotor assumed to be connected to the primary part near its center of mass, and whose spin axis is nominally parallel to the $\bar{b}_2$ body axis, and 3) a pendulous-type nutation damper which is attached to the main part and constrained to move in a plane a distance ℓ above the $\bar{b}_1, \bar{b}_3$ plane (determined by the body axes perpendicular to the symmetry axis, $\bar{b}_2$). The damper is hinged about a torsion wire support which offers a restoring torque in addition

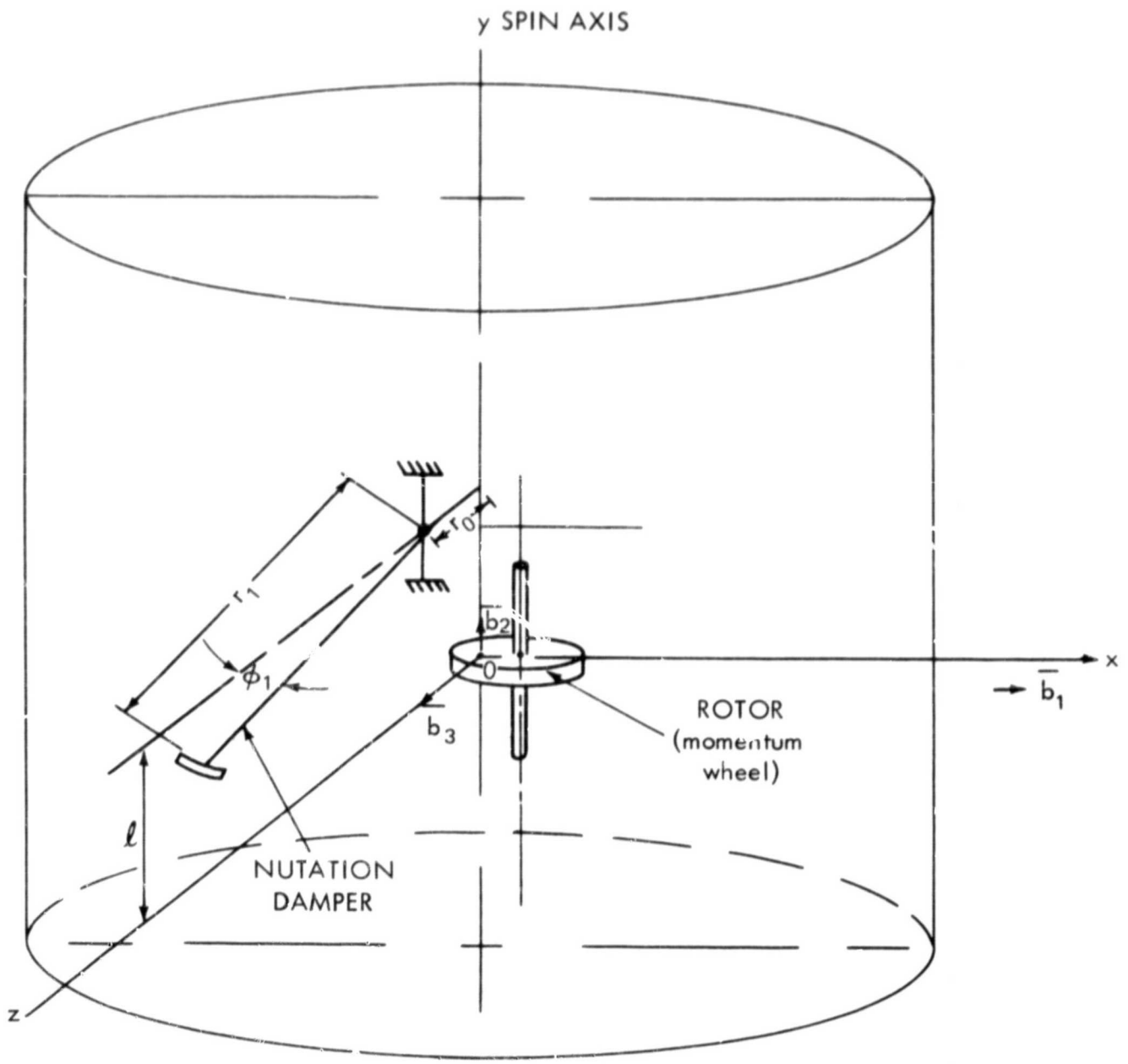

Figure 1. Elements of SAS-A Attitude Control System

to the dissipative torque associated with the damper motion. (A recent paper describes the design objectives and functional description of this damping system.[4]) In addition the rotor is assumed to have two degrees of flexural freedom with respect to the hub. In other words the plane of the rotor disc is allowed to deviate through small angular deflections from its nominal orientation which is parallel to the x, z plane.

A. Equations of Motion

The development of the equations of motion follows that of Reference 1, except now it is necessary to reformulate the expression for the kinetic energy of the rotor. The rotor is assumed to be spinning with a constant relative angular velocity magnitude, s, with respect to the main spacecraft. The nominal direction of the rotor spin axis is the direction of the $\bar{b}_2$ unit vector.

For the development of the rotor kinetic energy consider an incremental mass, dm_R, on the rotor disc which has a displacement coordinate y_R from the nominal rotor plane (Figure 2). The b_1', b_2', b_3' unit vectors are fixed to the nominal plane of the wheel and rotating with it. It has been assumed that the rotor is attached at or very near the center of mass of the main spacecraft-damper system. Neglecting any offset between the attachment point and the system mass center, the position vector of dm_R relative to the c.m. can be expressed for very small y displacement by:

$$\bar{r} \cong r \sin\phi\, \bar{b}_1' + y\, \bar{b}_2' + r \cos\phi\, \bar{b}_3' \qquad (1)$$

where ϕ is the position angle of the projection of dm_R on the plane of the undeflected wheel disc and does not vary with time. Utilizing the relationship between the time rates of change of a vector in an inertial and rotating system, the inertial velocity of dm_R relative to 0 can be expressed

$$\bar{v}_0 = \left(\omega_2' r \cos\phi - \omega_3' y_R\right)\bar{b}_1' + \left(\dot{y}_R + \omega_3' r \sin\phi - \omega_1' r \cos\phi\right) \bar{b}_2'$$

$$+ \left(\omega_1' y_R - \omega_2' r \sin\phi\right) \bar{b}_3' \qquad (2)$$

where ω_i' are the inertial angular velocity components of the rotor.

Sen and Fleisher[3] proceed to differentiate Equation (2) again with respect to time and obtain, from force and moment considerations, the two equations of motion for a wheel having two degrees of flexural freedom with respect to the hub under

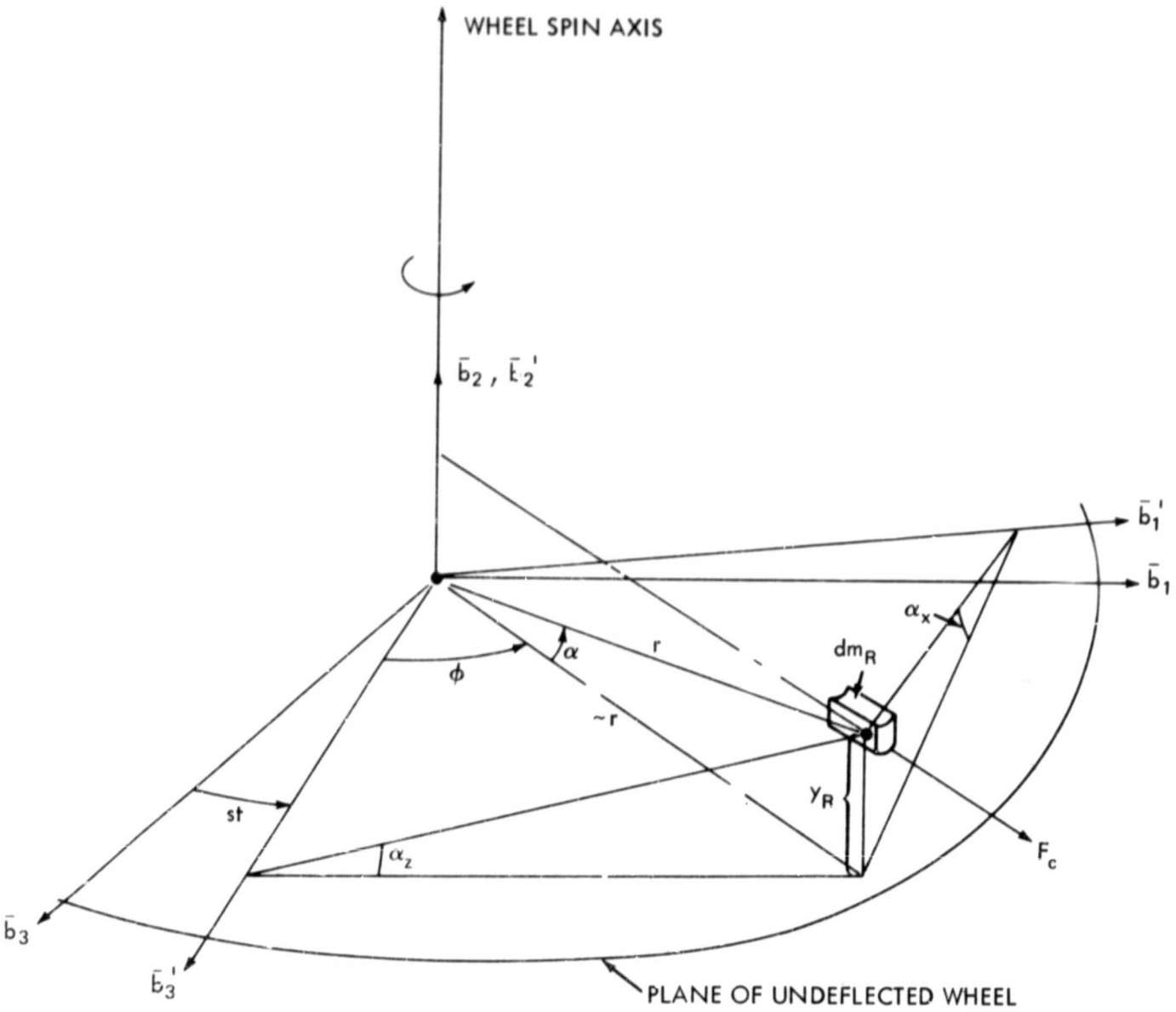

Figure 2. Momentum Wheel Deflection Geometry

suitable assumptions of small deflections. Because it is of interest here to determine the complete rotational equations of motion for the system, we will proceed to develop an expression for the kinetic energy of the rotor.

The kinetic energy of the incremental mass dm_R may be expressed as:

$$dT = \frac{1}{2} \bar{v}_0 \cdot \bar{v}_0 \, dm_R \qquad (3)$$

If it is assumed that the rotor has two degrees of flexural freedom with respect to the hub, i.e. α_z deflection about the $\bar{b}_3'$ axis and α_x deflection about $\bar{b}_1'$, then the displacement coordinate y_R can be written in terms of the flexure angles as:

$$y_R \cong r \sin\phi\, \alpha_z - r \cos\phi\, \alpha_x \tag{4}$$

for small deflections when the arc length can be approximated by the tangent. (For the general case of large deflections the position of dm_R would have to be expressed in terms of spherical coordinates or an Euler angle sequence.) The differential mass can be related to the unit disc thickness, h, and uniform density, ρ, according to:

$$dm_R = \rho h r\, dr\, d\phi \tag{5}$$

After substituting Equations (2), (4), and (5) into Equation (3) and integrating over the wheel volume,

$$T_{ROTOR} = \frac{1}{2}\left[I_{R_2}\left(\omega_2' + s\right)^2 + I_{R_1}\left(\omega_1'^2 + \omega_3'^2\right)\right]$$

$$+ \frac{I_{R_1}}{2}\left[\dot{\alpha}_z^2 + \dot{\alpha}_x^2 + 2\omega_3'\dot{\alpha}_z - 2\omega_1'\dot{\alpha}_x - 2\omega_1'\omega_2'\alpha_z - 2\omega_3'\omega_2'\alpha_x\right.$$

$$\left. + \left(\omega_1'^2 + \omega_3'^2\right)\left(\alpha_z^2 + \alpha_x^2\right)\right] \tag{6}$$

where

$$I_{R_1} = m_R\left(d_1^2 + d_2^2\right)/4\,; \qquad I_{R_2} = 2\,I_{R_1}$$

and m_R is the mass of the rotor rim; d_1, d_2 are the inner and outer radius of the rim, respectively.

By writing the ω_i' in terms of the ω_i (see Figure 2), Equation (6) may be expanded in terms of the spacecraft body angular rates to yield:

$$T_{ROTOR} = \frac{1}{2}\left[I_{R_2}(\omega_2 + s)^2 + I_{R_1}(\omega_1^2 + \omega_3^2)\right]$$

$$+ \frac{I_{R_1}}{2}\Big[2\dot{\alpha}_z(\omega_3 \cos st + \omega_1 \sin st) - 2\dot{\alpha}_x(-\omega_3 \sin st + \omega_1 \cos st)$$

$$- 2(-\omega_3 \sin st + \omega_1 \cos st)(\omega_2 + s)\alpha_z$$

$$- 2(\omega_3 \cos st + \omega_1 \sin st)(\omega_2 + s)\alpha_x$$

$$+ (\omega_1^2 + \omega_3^2)(\alpha_z^2 + \alpha_x^2) + \dot{\alpha}_z^2 + \dot{\alpha}_x^2\Big] \quad (7)$$

In the limiting case, if the rotor is assumed to be completely rigid without flexural freedom with respect to the hub, $\alpha_z = \dot{\alpha}_z = \alpha_x = \dot{\alpha}_x = 0$, and,

$$T_{ROTOR} = \frac{1}{2}\left[I_{R_2}(\omega_2 + s) + I_{R_1}(\omega_1^2 + \omega_3^2)\right] \quad (8)$$

Equation (8) is seen to be identical to Equation (1) of Reference 1.

An additional centrifugal force potential exists which is associated with conservative forces tending to restore the deflected rotor rim to the nominal $\bar{b}_1$, $\bar{b}_3$ plane. With the aid of Figure 2 it can be seen that the centrifugal force acting on dm_R due to the rotation about the $\bar{b}_2$ axis can be approximated, for $\alpha \ll 1$ and $y \ll r$, by

$$F_c = dm_R\, r(\omega_2 + s)^2 \quad (9)$$

The component of F_c tending to accelerate dm_R toward the plane of the undeflected wheel is:

$$F_{c_\alpha} = F_c \sin\alpha \approx r\,\alpha\, dm_R \left(\omega_2 + s\right)^2 \tag{10}$$

But for small deflections $r\alpha \approx y_R$, so that

$$F_{c_\alpha} \approx r\left(\alpha_z \sin\phi + \alpha_x \cos\phi\right)\left(\omega_2 + s\right)^2 dm_R \tag{11}$$

To obtain the potential, consider the work done by F_{c_α} through the differential distance $dy_R \cos\alpha \approx dy_R = r\left(\sin\phi\, d\alpha_z + \cos\phi d\alpha_x\right)$,

$$dW = \overline{F}_{c_\alpha} \cdot \overline{dy}_R \tag{11}$$

After performing the multiple integration, and recalling the relationship that $I_{R_1} = m_R\left(d_1^2 + d_2^2\right)/4$, the following expression is obtained:

$$V_{ROTOR_c} = \frac{I_{R_1}}{2}\left(\omega_2 + s\right)^2\left(\alpha_x^2 + \alpha_z^2\right) \tag{12}$$

If it is now assumed that the wheel dissipative forces vary linearly with the flexural angular rates $\dot{\alpha}_x$ and $\dot{\alpha}_z$, these forces can be derived from a Rayleigh dissipation function, $\mathfrak{F}$, similar to that given in Reference 1, which has the form:

$$\mathfrak{F} = \frac{1}{2}\left[k_1 \dot{\phi}_1^2 + k_R\left(\dot{\alpha}_x^2 + \dot{\alpha}_z^2\right)\right] \tag{13}$$

where k_R is the equivalent linear viscous damping constant of the rotor. Wheel damping tests performed at the Applied Physics Laboratory verify that, to first order, there is a linear relationship between wheel dissipative forces and the flexural angular rates. (Likins et al.[5] have recently discussed some of the difficulties which can result due to damping nonlinearities in dual spin systems and have also presented a technique of relating an equivalent linear viscous damping coefficient to the actual nonlinear damping.)

In addition to the centrifugal restoring forces on the rotor, there is also a restoring effect due to the stiffness of the rotor material itself. For small deflections and homogeneous wheel material these forces can be obtained from the following potential energy expression:

$$V_{ROTOR} = \frac{1}{2} K_R \left(\alpha_z^2 + \alpha_x^2\right) + \frac{1}{2} I_{R_1} \left(\omega_2 + s\right)^2 \left(\alpha_z^2 + \alpha_x^2\right) \tag{13}$$

where K_R is the restoring spring constant of the rotor and dependent on the EI_R of the rotor material.

The complete potential energy for the system now can be expressed as:

$$V = \frac{1}{2} \left\{ K \phi_1^2 + \left[K_R + I_{R_1} \left(\omega_2 + s\right)^2 \right] \left(\alpha_z^2 + \alpha_x^2\right) \right\} \tag{14}$$

whereas the complete rotational kinetic energy for the system is the sum of main body, nutation damper, and rotor components:

$$T = T_M + T_m + T_R \tag{15}$$

and the rather lengthy expression for $T_M + T_m$ is presented in Reference 1 (in report form).

The equations of motion for the system can be expressed in terms of the quasi-coordinates ($\omega_1, \omega_2, \omega_3$), the angle swept out by the pendulous nutation damper (ϕ_1), and the rotor deflection angles (α_x, α_z) according to:[6]

$$\frac{d}{dt}\left(\frac{\partial L}{\partial \omega_1}\right) - \omega_3 \frac{\partial L}{\partial \omega_2} + \omega_2 \frac{\partial L}{\partial \omega_3} = L_1$$

$$\frac{d}{dt}\left(\frac{\partial L}{\partial \omega_2}\right) - \omega_1 \frac{\partial L}{\partial \omega_3} + \omega_3 \frac{\partial L}{\partial \omega_1} = L_2$$

$$\frac{d}{dt}\left(\frac{\partial L}{\partial \omega_3}\right) - \omega_2 \frac{\partial L}{\partial \omega_1} + \omega_1 \frac{\partial L}{\partial \omega_2} = L_3$$

$$\frac{d}{dt}\left(\frac{\partial T}{\partial \dot{\phi}_1}\right) - \frac{\partial T}{\partial \phi_1} + \frac{\partial \mathfrak{I}}{\partial \dot{\phi}_1} = -\frac{\partial V}{\partial \phi_1}$$

$$\frac{d}{dt}\left(\frac{\partial T}{\partial \dot{\alpha}_x}\right) - \frac{\partial T}{\partial \alpha_x} + \frac{\partial \mathfrak{I}}{\partial \dot{\alpha}_x} = -\frac{\partial V}{\partial \alpha_x}$$

$$\frac{d}{dt}\left(\frac{\partial T}{\partial \dot{\alpha}_z}\right) - \frac{\partial T}{\partial \alpha_z} + \frac{\partial \mathfrak{I}}{\partial \dot{\alpha}_z} = -\frac{\partial V}{\partial \alpha_z} \qquad (16)$$

Numerical studies with the previously developed nonlinear equations of motion[1] indicate that whenever the transverse components of main body angular velocities are the same order as ω_2, the nutation damper motion is characterized by large amplitudes and eventually makes contact with the mechanical stops placed on the spacecraft to limit ϕ_1 displacement to ±20 degrees. Because a stability analysis of such a discontinuous system is beyond the scope of the present analysis, it was decided to expand Equations (16) under the assumptions that $\omega_i\ \omega_2 < 1$, $\dot{\alpha}_{x,z} < 1$, $\dot{\phi}_1 < 1$, $\phi_1 < 1$, and $\alpha_{x,z} < 1$.

The following first order nonlinear equations of motion result:

$$\bar{B}\dot{\omega}_2 + \omega_1 \omega_3 (\bar{A} - \bar{C}) + m r_1 (r_1 + r_0) \ddot{\phi}_1 = L_2 \qquad (17)$$

$$\bar{A}\dot{\omega}_1 + \omega_2 \omega_3 (\bar{C} - \bar{B}) - \omega_3 I_{R_2} s - 2m\omega_2 r_1 \frac{\ell M}{\bar{M}} \dot{\phi}_1$$

$$+ I_{R_1} \left\{ \left[\ddot{\alpha}_z + (\omega_2 + s)^2 \alpha_z \right] \sin st - \left[\ddot{\alpha}_x + (\omega_2 + s)^2 \alpha_x \right] \cos st \right\} = L_1 \qquad (18)$$

$$\bar{C}\dot{\omega}_3 + \omega_1 \omega_2 (\bar{B} - \bar{A}) + \omega_1 I_{R_2} s - m r_1 \frac{\ell M}{\bar{M}} \ddot{\phi}_1 + m\omega_2^2 r_1 \frac{\ell M}{\bar{M}} \phi_1$$

$$+ I_{R_1} \left\{ \left[\ddot{\alpha}_z + (\omega_2 + s)^2 \alpha_z \right] \cos st + \left[\ddot{\alpha}_x + (\omega_2 + s)^2 \right] \sin st \right\} = L_3 \qquad (19)$$

$$m r_1^2 \left(1 - \frac{m}{\bar{M}}\right) \ddot{\phi}_1 - m r_1 \frac{\ell M}{\bar{M}} \dot{\omega}_3 + m r_1 \left(r_0 + r_i\right) \dot{\omega}_2 + \omega_2^2 m r_1 \left(r_0 + \frac{m r_1}{\bar{M}}\right) \phi_1$$

$$+ m\omega_2 r_1 \frac{\ell M \omega_1}{\bar{M}} = - k\dot{\phi}_1 - K\phi_1 \quad (20)$$

$$I_{R_1} \ddot{\alpha}_z + k_R \dot{\alpha}_z + \left[K_R + I_{R_1} \left(\omega_2 + s\right)^2\right] \alpha_z$$

$$+ I_{R_1} \left\{\left[\dot{\omega}_1 - \left(\omega_2 + 2s\right) \omega_3\right] \sin st + \left[\dot{\omega}_3 + \left(\omega_2 + 2s\right) \omega_1\right] \cos st\right\} = 0 \quad (21)$$

$$I_{R_1} \ddot{\alpha}_x + k_R \dot{\alpha}_x + \left[K_R + I_{R_1} \left(\omega_2 + s\right)^2\right] \alpha_x$$

$$+ I_{R_1} \left\{\left[\dot{\omega}_3 + \left(\omega_2 + 2s\right) \omega_1\right] \sin st - \left[\dot{\omega}_1 - \left(\omega_2 + 2s\right) \omega_3\right] \cos st\right\} = 0 \quad (22)$$

where the super barred inertia terms have main body, rotor and nutation damper components:

$$\bar{A} = I_{b_1} + I_{R_1} + I_{d_1}; \quad \bar{B} = I_{b_2} + I_{R_2} + I_{d_2}; \quad \bar{C} = I_{b_3} + I_{R_3} + I_{d_3}$$

For small displacements of the nutation damper, and for $m/M <<< 1$, the system center of mass shift due to this motion wili be very small and is not included in these equations. It is assumed, of course, that the satellite is statically balanced in equilibrium when $\phi_1 = 0$.

B. Stability Criteria

Equations (17)—(22) when linearized about the equilibrium motion: $\omega_2 = \Omega$,

$$\omega_1 = \omega_3 = \phi_1 = \alpha_x = \alpha_z = \dot{\omega}_1 = \dot{\omega}_3 = \dot{\phi}_1 = \dot{\alpha}_x = \dot{\alpha}_z = 0$$

would represent a set of nonautonomous differential equations with both constant and periodic coefficients. The stability of such a system could be analyzed using Floquet theory similar to the treatment of Mingori.[2] The application of Floquet theory for this problem would necessitate the use of a digital computer to study

the stability point by point by varying different satellite and rotor inertia, spin, and damping system parameters in a systematic manner.

In an effort to investigate the stability of this system analytically, the technique employed by Flatley[7] in his doctoral dissertation, and applied to the earlier problem of Mingori, was applied.

It is assumed that the effects of the nutation damper and wheel deflections relative to the hub are small perturbations on the nominal rigid body motion of the torque-free dual spin system. The "zeroth order" equations which represent the reference motion, or unperturbed state, can be obtained by assuming that terms such as mr_1^2 and $mr_1 \ell$ are much smaller than main body inertia terms A, B, and C, and also that $I_{R_1} \ll$ A, B, or C. The SAS-A satellite is almost perfectly symmetrical about the $\bar{b}_2$ axis so that A = C; also under the approximations mentioned above $A = \bar{A}$, $B = \bar{B}$. The resulting zeroth order equations corresponding to Equations (17), (18), and (19) with $L_1 = L_2 = L_3 = 0$ are:

$$B\dot{\omega}_2 = 0 \tag{23}$$

$$A\dot{\omega}_1 - \omega_2 \omega_3 (B - A) - \omega_3 I_{R_2} s = 0 \tag{24}$$

$$A\dot{\omega}_3 + \omega_1 \omega_2 (B - A) + \omega_1 I_{R_2} s = 0 \tag{25}$$

Equation (23) has the solution $\omega_2 = \Omega$, which when substituted into Equations (24) and (25) yields:

$$\dot{\omega}_1 - \lambda\omega_3 = 0 \tag{26}$$

$$\dot{\omega}_3 + \lambda\omega_1 = 0 \tag{27}$$

where

$$\lambda = \left[(B - A)\Omega + I_{R_2} s\right] / A$$

The solution to Equations (26) and (27) has the form

$$\omega_1 = \omega \sin \lambda t \tag{28}$$

$$\omega_3 = \omega \cos \lambda t \tag{29}$$

where $\omega = \omega_3 (0)$, the value of ω_3 at some reference time.

Thus for the unperturbed reference motion of the main body, the angular velocity component along the nominal spin axis is a constant while the vector sum of the transverse components rotates around $\bar{b}_2$ with the nutation frequency λ. If $s = 0$, the system reduces to the classical problem of the spinning symmetrical rigid body.

To determine the first order damper and wheel deflection motions all terms linear in m and I_{R_1} are retained. After substitution of the zeroth order main body angular velocities into the equations for the damper and wheel deflections, the following equations result:

$$m r_1^2 \ddot{\phi}_1 + k \dot{\phi}_1 + \left(K + m r_1 r_0 \Omega^2\right) \phi_1 = - m r_1 \Gamma \omega \left[(\lambda + \Omega) \sin \lambda t\right] \tag{30}$$

$$I_{R_1} \ddot{\alpha}_z + k_R \dot{\alpha}_z + \left[K_R + I_{R_1} (s + \Omega)^2\right] \alpha_z = - I_{R_1} \omega \left[(\lambda - \Omega - 2s) \sin (s - \lambda) t\right] \tag{31}$$

$$I_{R_1} \ddot{\alpha}_x + k_R \dot{\alpha}_x + \left[K_R + I_{R_1} (s + \Omega)^2\right] \alpha_x = I_{R_1} \omega \left[(\lambda - \Omega - 2s) \cos (s - \lambda) t\right] \tag{32}$$

Equations (31) and (32) correspond identically to the approximate equations of motion for the wheel deflections as derived by Sen and Fleisher.[3]

The steady state solutions to Equations (30)—(32) can be written in the form:

$$\phi_{1_{ss}} = C_1 \sin \lambda t + C_2 \cos \lambda t \tag{33}$$

$$\alpha_z = C_3 \sin (s - \lambda) t + C_4 \cos (s - \lambda) t \tag{34}$$

$$a_x = C_5 \sin(s-\lambda)\,t + C_6 \cos(s-\lambda)\,t \qquad (35)$$

where

$$C_1 = -mr_1 \Gamma\omega(\lambda+\Omega)\left[K + mr_1\left(r_0\Omega^2 - r_1\lambda^2\right)\right]\Big/D_1$$

$$C_2 = mr_1 \Gamma k\omega\lambda(\lambda+\Omega)\Big/D_1$$

$$C_3 = -I_{R_1}\omega(\lambda-\Omega-2s)\left\{K_R + I_{R_1}\left[(s+\Omega)^2 - (s-\lambda)^2\right]\right\}\Big/D_2$$

$$C_4 = I_{R_1}\omega(\lambda-\Omega-2s)(s-\lambda)\,k_R\Big/D_2$$

$$C_5 = C_4$$

$$C_6 = -C_3$$

and

$$D_1 = \left[K + mr_1\left(r_0\Omega^2 - r_1\lambda^2\right)\right]^2 + (k\lambda)^2$$

$$D_2 = \left\{K_R + I_{R_1}\left[(s+\Omega)^2 - (s-\lambda)^2\right]\right\}^2 + (s-\lambda)^2 k_R^2$$

In the absence of the external torques the total angular momentum vector of the system about an axis passing through the system center of mass (point 0) remains time invariant. If the nutation angle, γ, is defined as the angle between the $\bar{b}_2$ axis and the total angular momentum vector of the system, $\bar{H}$, then

$$H_{0_2} = H_0 \cos\gamma \qquad (36)$$

where $H_O = |\bar{H}_O|$, $H_{O_2} = |H_{O_2}\,\bar{b}_2|$. The component H_{O_2} may be obtained by expanding the following:

$$H_{O_2} = B\omega_2 + \left(\bar{r}_{m_0} \times \bar{P}_{m_0}\right) \cdot \bar{b}_2 + \left[\int_{m_R} \left(\bar{r}_{dm_0} \times \bar{v}_0\right) dm\right] \cdot \bar{b}_2 \qquad (37)$$

where $\bar{P}_{m_O}$ is the linear momentum of the nutation damper about an axis through 0, $\bar{v}_0$ is given by Equation (2), m is the pendulum end mass, and m_R is the mass of the rotor. After expansion of Equation (37) and neglecting terms involving $m^2/\bar{M} << m$

$$H_{O_2} = B\omega_2 + m\left\{\left(r_1^2 + r_0^2 + 2r_0\, r_1 \cos\phi_1\right)\left(\omega_2 + \dot{\phi}_1\right)\right.$$

$$+ \Gamma\left[-\omega_1\, r_1 \sin\phi_1 - \omega_3\left(r_0 + r_1\cos\phi_1\right)\right]$$

$$\left. - \dot{\phi}_1\left(r_0^2 + r_1\, r_0 \cos\phi_1\right)\right\} + I_{R_2}\left(\omega_2 + s\right)$$

$$- I_{R_1}\left[a_z\left(-\omega_3 \sin st + \omega_1 \cos st\right)\right.$$

$$\left. + a_x\left(\omega_3 \cos st + \omega_1 \sin st\right)\right] = H_O \cos\gamma \qquad (38)$$

By differentiating both sides of Equation (38) with respect to time, and substituting for $\dot{\omega}_2$ from the completely nonlinear form of Equation (17), the following expression is obtained for $\dot{H}_{O_2}$:

$$-I\sin\gamma\dot{\gamma} = -mr_0\, r_1\, \dot{\phi}_1^2 \sin\phi_1$$

$$+ m\Gamma r_1\left[\omega_2\,\omega_3 \sin\phi_1 - \omega_2\,\omega_1 \cos\phi_1 + \dot{\phi}_1\left(-\omega_1 \cos\phi_1 + \omega_3 \sin\phi_1\right)\right]$$

$$+ I_{R_1} \left\{ \left[\omega_3 \cos st + \omega_1 \sin st \right] \left[a_z (\omega_2 + s) + \dot{a}_x \right] \right.$$

$$+ \left[\omega_3 \sin st - \omega_1 \cos st \right] \left[a_x (\omega_2 + s) - \dot{a}_z \right]$$

$$\left. + \dot{\omega}_2 (a_z^2 + a_x^2) + 2(\omega_2 + s)(a_z \dot{a}_z + a_x \dot{a}_x) \right\} \quad (39)$$

Equation (39) is an exact expression except for the limitation on the magnitude of m. If $m = I_{R_1} = 0$, the cone angle γ is a constant of the motion.

To analytically express the first order perturbation of the cone angle, the zeroth order expressions for main body rates: $\omega_1 = \omega \sin \lambda t$, $\omega_2 = \Omega$, $\omega_3 = \omega \cos \lambda t$ are substituted into Equation (39) to yield:

$$-H \sin \gamma \dot{\gamma} = -m r_0 r_1 \dot{\phi}_1^2 \sin \phi_1$$

$$+ m \Gamma r_1 \omega \left\{ \left[\Omega \cos \lambda t \sin \phi_1 - \Omega \sin \lambda t \cos \phi_1 \right] \right.$$

$$\left. + \left[\dot{\phi}_1 (-\sin \lambda t \cos \phi_1 + \cos \lambda t \cdot \sin \phi_1) \right] \right\}$$

$$+ I_{R_1} \omega \left\{ \left[\cos (s - \lambda) t \right] \left[a_z (\Omega + s) + \dot{a}_x \right] \right.$$

$$\left. + \left[\sin (s - \lambda) t \right] \left[a_x (\Omega + s) - \dot{a}_z \right] \right\} \quad (40)$$

Substitution for a_z and a_x, Equations (34) and (35), would produce $\sin^2$ and $\cos^2$ terms in $(s - \lambda) t$, while substitution of ϕ_1, Equation (33), would produce $\sin^2$ and $\cos^2$ terms and higher order terms in λt, after $\sin \phi_1$ and $\cos \phi_1$ terms in Equation (40) have been expressed in series form. With the use of trigonometric identities, the squared terms may be eliminated, the higher order terms reduced, so that the resulting equation would contain only constants and sinusoidal oscillatory terms.

Following Flatley,[7] in the spirit of the method of averaging, the systematic change of γ is considered to be influenced mainly by the constant terms, with the sinusoidal terms contributing only small perturbations of γ about some average value.

After retaining only the constant terms in the above averaging process, the secular motion of the nutation angle can be described by:

$$\dot{\gamma} = -\frac{\omega}{2H \sin\gamma}\left[mr_1 \Gamma(\Omega+\lambda) C_2 + I_{R_1}(2s-\lambda+\Omega)\left(C_4 + C_5\right)\right] \tag{41}$$

Substituting the values of C_2, C_4, and C_5 from Equations (33)—(35), and approximating $H \sin\gamma$ by the transverse angular momentum of the unperturbed motion, Equation (41) becomes:

$$\dot{\gamma} = -\frac{H \sin\gamma}{2A^2}\left[\frac{\left(mr_1 \Gamma\right)^2 (\Omega+\lambda)^2 k\lambda}{D_1} - \frac{2I_{R_1}^2 (2s-\lambda+\Omega)^2 k_R (s-\lambda)}{D_2}\right] \tag{42}$$

where

$$\omega = H \sin\gamma / A$$

$$\Omega = \left[H \cos\gamma - I_{R_2} s\right] / B$$

and

$$\lambda = \left[(B-A) H \cos\gamma + A I_{R_2} s\right] / BA$$

Equation (42) has the form $\dot{\gamma} = f(\gamma)$, and equilibrium will be possible whenever $f(\gamma) = 0$. Stability at an equilibrium point, γ_0, requires $f\left(\gamma_0\right) = 0$ and $df/d\gamma\big|_{\gamma_0} < 0$. Thus, the attitude behavior of this ninth order, nonlinear system is represented by the single first order differential equation, Equation (42).

If $\dot{\gamma} = f(\gamma) = F(\gamma) \sin\gamma$, then an equilibrium state will always exist at $\gamma_0 = 0$, $\gamma_0 = \pi$, and, possibly at intermediate nutation angles, if $F(\gamma_0) = 0$. For this application the nutation angle is bounded by $0 \leq \gamma \leq \pi$. For stability, from consideration of $f'(\gamma_0) < 0$, at $\gamma_0 = 0$, it is necessary that $F(0) < 0$; at $\gamma_0 = \pi$, it is necessary that $F(\pi) > 0$; at γ_0, it is necessary that, $F(\gamma_0) = 0$ and $F'(\gamma_0) < 0$.

C. Special Case-Damper on Spacecraft Only

For the case where there is only damping present on the main part of the spacecraft and no damping on the wheel,

$$F = -\frac{H}{2A^2 D_1}\left[(mr_1\Gamma)^2 (\Omega+\lambda)^2 \cdot k\lambda\right] \tag{43}$$

when $k = 0$, or $\ell = \Gamma = 0$, or $r_1 = 0$, then $F = 0$ and the system is unstable for all values of γ_0. The conditions that, for stability at $\gamma_0 = 0$, $k > 0$, $\ell > 0$, $r_1 > 0$ are part of the necessary and sufficient stability criteria previously derived by the methods of Routh-Hurwitz for the case of spacecraft damping only.[1] Assuming these conditions are satisfied, the sign of F is clearly determined by the sign of $-\lambda$. Therefore, for stability at $\gamma_0 = 0$, $-\lambda > 0$, or $\lambda > 0$, or

$$\lambda\big|_{\gamma_0 = 0} = \frac{(B-A)\, H_{\gamma_0} + AI_{R_2}\, s}{AB} > 0 \tag{44}$$

Condition (44) can be shown to be equivalent to:

$$\bar{B} + I_{R_2}\left(s/\Omega\right) - \bar{A} > 0 \tag{45}$$

within the assumptions previously made regarding A, $\bar{A}$, and B, $\bar{B}$. Condition (45) is equivalent to inequality (16) of Reference 1, resulting from the Routh-Hurwitz analysis.

It is apparent that from consideration of Equation (43), the necessary and sufficient stability criterion, (18), of Reference 1, repeated here:

$$\frac{r_0}{r_1} + \frac{m}{\bar{M}} + \bar{K} > \frac{m\Gamma^2}{\bar{B} - \bar{A} + I_{R_2} s/\Omega} \tag{46}$$

is not apparent. This can possibly be explained by the fact that $m/\bar{M}$ and $m\Gamma^2$ (for small or moderate ℓ) are higher order terms when compared with, $\bar{A}$, $\bar{B}$, or $I_{R_2} s/\Omega$, as in the present analysis. In practical application, condition (46) limits the maximum height of the damper plane for a given set of main body inertias, nutation damping system parameters, and ratio of s/Ω.

From consideration of Ineq. (44), the line $\lambda_0 = 0$ or $s/\Omega_0 = (A - B)/I_{R_2}$, divides the initial state plane into the regions $\lambda_0 > 0$, $\lambda_0 < 0$. The region: $\lambda_0 > 0$ is stabilizing for values of $\gamma_0 = 0$, whereas the region: $\lambda_0 < 0$ describes stability for $\gamma_0 = \pi$. Furthermore, the line: $B\Omega_0 + I_{R_2} s = H \cos \gamma = 0$ divides the (Ω_0, s) plane into regions describing $\gamma_0 = 0$, and $\gamma_0 = \pi$. Superimposing the two results, the following stability diagram can be constructed in the (Ω_0, s) plane (Figure 3), where the shaded regions indicate stability.

As Flatley indicates[7] a useful alternate form of this stability diagram is obtained by letting: $q = \bar{B}/\bar{A} \approx B/A$, and $q' = I_{R_2}/\bar{A} \approx I_{R_2}/A$. The boundary line, $s/\Omega_0 = (A - B)/I_{R_2}$ becomes $1 = q + q' s/\Omega_0$ and the boundary line; $B\Omega_0 + I_{R_2} s = 0$ becomes $q + q' s/\Omega_0 = 0$. The transformed stability diagram appears in Figure 4, where the physically meaningful values of q are restricted to $q' < q < 2$. Unless the momentum wheel is deliberately designed to spin opposite to the sense of the main body angular momentum vector, the physically meaningful values of s/Ω_0 are to the right of the q axis. Figure 4 is identical to a result obtained by Mingori[2] using some of the Routhian stability boundaries.

A critical value of rotor spin[7] occurs when only one stable equilibrium nutation angle exists and $\gamma_0 = \pi$ is unstable. This value may be obtained by setting $\lambda = 0$ when $\gamma_0 = \pi$, yielding

$$s_{crit} = (B - A) H_0/AI_{R_2} \tag{47}$$

When $s > s_{crit}$, at $\gamma_0 = \pi$, then λ becomes positive, and thus $F(\pi) < 0$; therefore, $\gamma_0 = \pi$ becomes a point of unstable equilibrium, i.e. a dual-spin satellite which

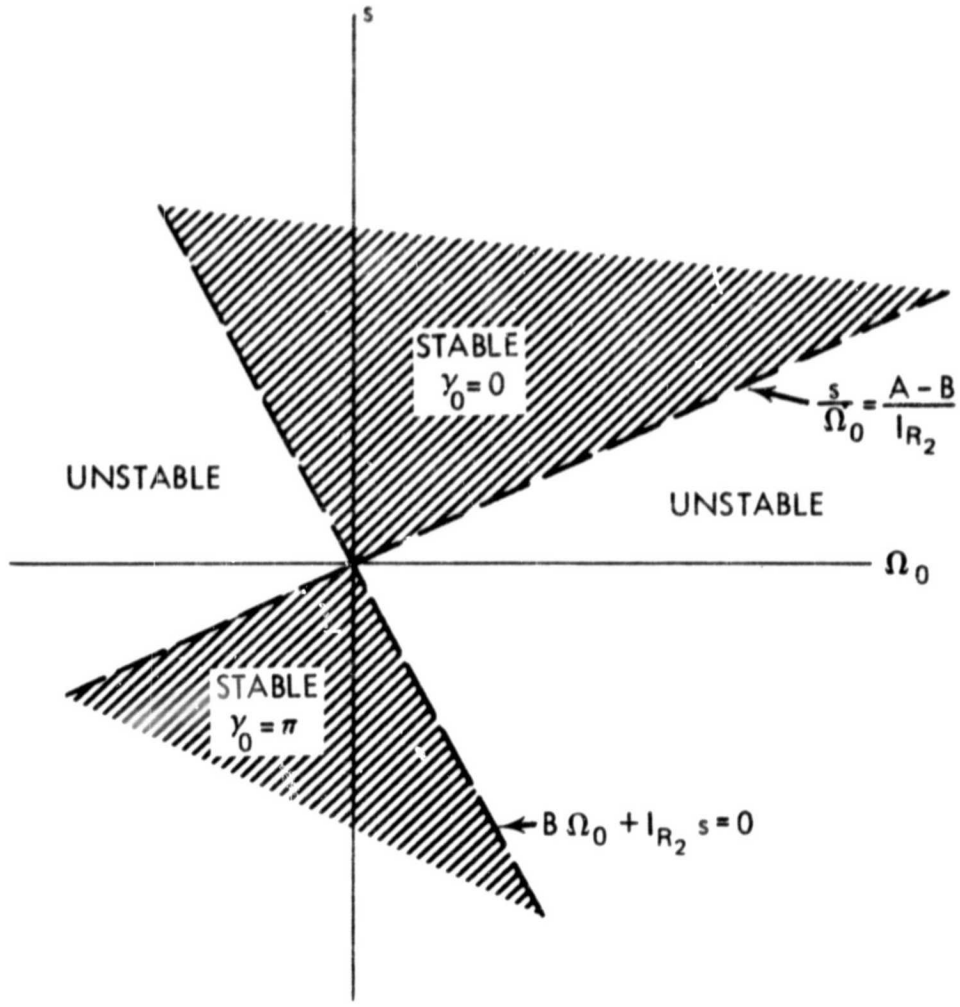

Figure 3. Stability Diagram With Damping Only on the Spacecraft

has inverted itself from its nominal pointing direction, will, in the presence of main body damping, tend to restore itself to the "upright" position.

D. Special Case-Damper on Momentum Wheel Only

If there is only damping present on the momentum wheel,

$$F = \frac{H}{A^2 D_2}\left[I_{R_1}^2 (2s - \lambda + \Omega)^2 k_R (s - \lambda)\right] \tag{48}$$

when $k_R = 0$, then $F = 0$, and the system is unstable for all values of γ_0. For this special case, if $k_R > 0$ and there is damping on the wheel, the sign of F is directly dependent on the sign of $(s-\lambda)$. An initial nutation angle of zero is stable if $(s - \lambda_0)$ is negative, while an initial nutation angle of 180° is stable if $(s - \lambda_0)$ is positive. Therefore, the line $\lambda_0 - s = 0$, or $s/\Omega_0 = (B - A)/(A - I_{R_2})$

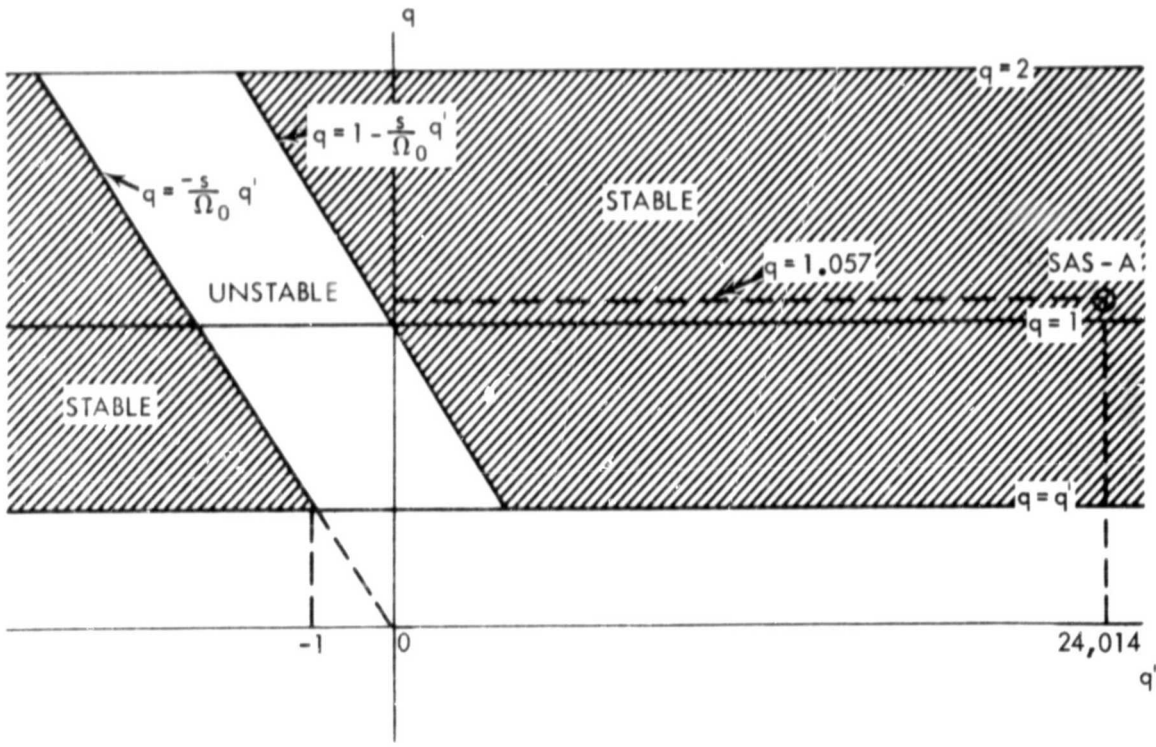

Figure 4. Stability Diagram in q, q′ Space With Damping Only on the Spacecraft

divides the s, Ω_0 plane into the two possible regions: $\lambda_0 - s > 0$ and $\lambda_0 - s < 0$. Recalling that the line $s/\Omega_0 = -B/I_{R_2}$ separates the Ω_0, s plane into the two regions corresponding to $\gamma_0 = 0$ and $\gamma_0 = \pi$ respectively, a stability diagram may be constructed (Figure 5).

Again this diagram may be reconstructed in terms of the nondimensional parameters q and q′, as before. The physically realistic values of q are given by: $q' < q < 2$. Figure 6 illustrates the alternate form of Figure 5 for the special case of wheel damping only.

E. Discussion of General Case

The general expression for time rate of change of nutation angle, (42), may be expressed as:

$$\dot{\gamma} = \frac{\omega^2}{2H \sin\gamma} \left[\frac{-(mr_1\Gamma)^2 (\Omega+\lambda)^2 k\lambda}{D_1} + \frac{2I_{R_1}^2 (2s - \lambda + \Omega) k_R (s-\lambda)}{D_2} \right] \qquad (49)$$

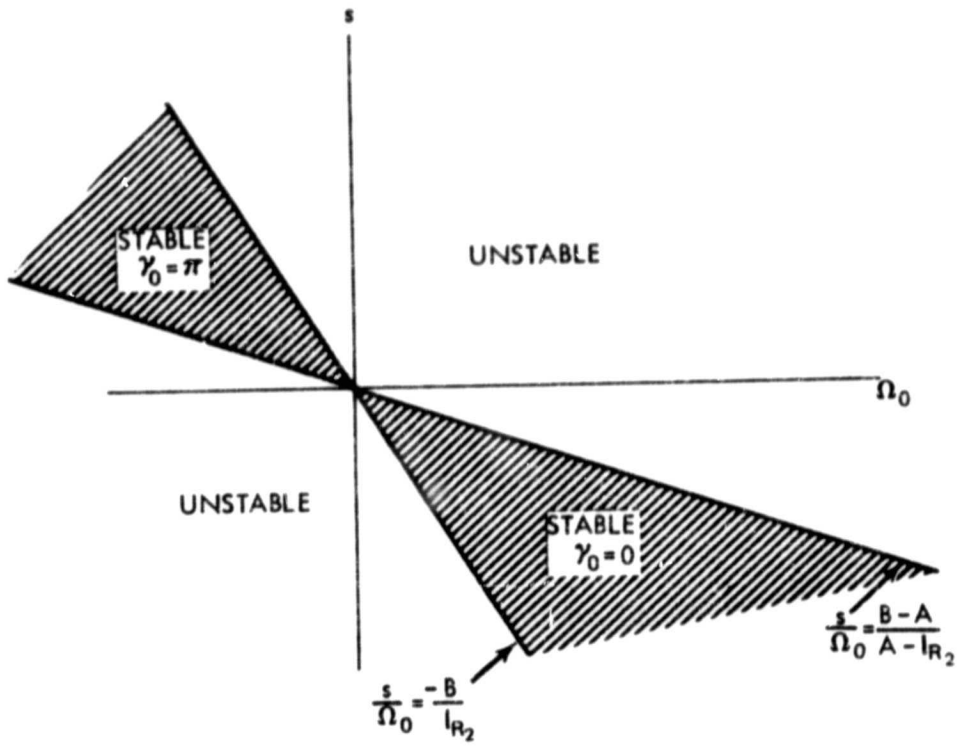

Figure 5. Stability Diagram With Damping Only on the Wheel

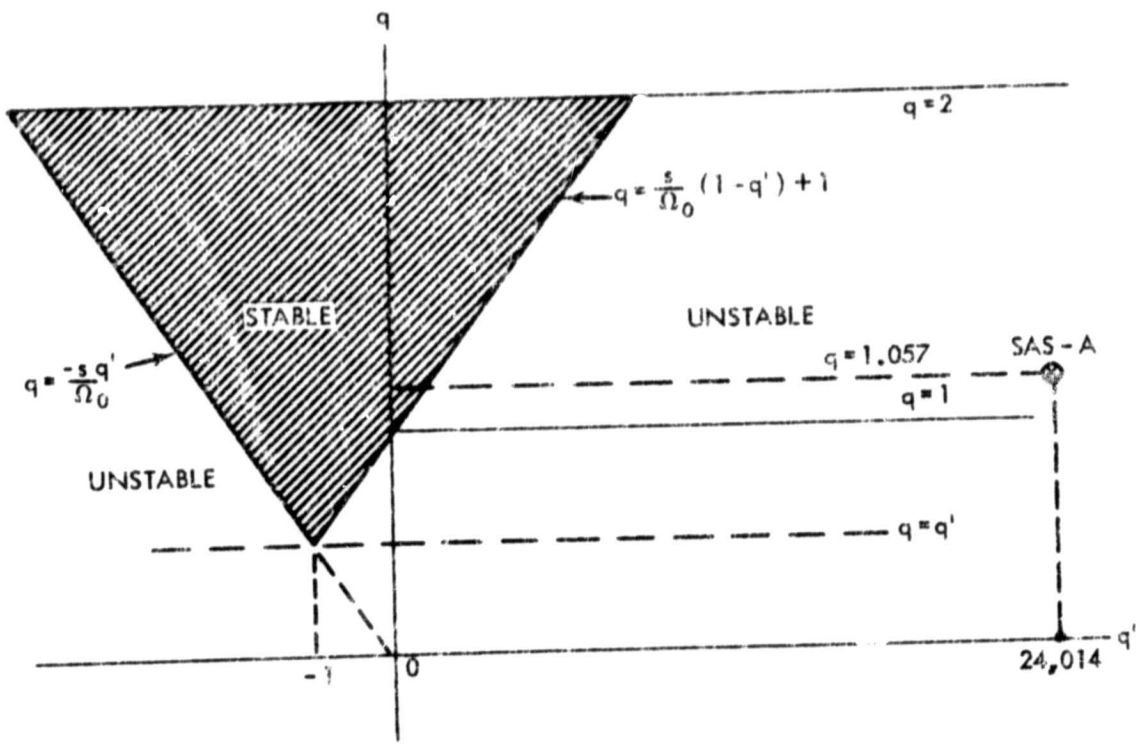

Figure 6. Stability Diagram in q, q' Space With Damping Only on the Wheel

after substituting $1/A^2 = \omega^2/H^2 \sin^2\gamma$. From this, necessary conditions for stability at the equilibrium positions of $\gamma_0 = 0$, and $\gamma_0 = \pi$ may be obtained by examining the sign of $F(\gamma_0)$, and at an intermediate position, γ_0, by examining the sign of $F'(\gamma_0)$ as explained earlier.

Likins[8] has previously derived attitude stability criteria for a dual spin spacecraft in terms of the average energy dissipation rates on both the wheel and the despun portion using an approximate energy sink analysis. In an effort to compare the form of Equation (49) with Likins' criteria the average energy dissipation rates were evaluated for the SAS-A dual spin system.

The average energy dissipation rate due to the action of the pendulous nutation damper is:

$$\dot{T}_{D_{ave}} = -k\dot{\phi}_{1_{ss_{ave}}}^2 \tag{50}$$

From Equation (33),

$$\dot{\phi}_{1_{ss}}^2 = \lambda^2\left(C_1^2\cos^2\lambda t - C_1 C_2 \sin 2\lambda t + C_2^2 \sin^2\lambda t\right) \tag{51}$$

In order to obtain $\dot{\phi}_{1_{ss_{ave}}}^2$, Equation (51) is averaged using the same procedure as before, by writing terms involving $\cos^2$ and $\sin^2$ in terms of constant terms and sinusoidal terms, and retaining only the constant terms in the averaging process. There results,

$$\dot{\phi}_{1_{ss_{ave}}}^2 = \frac{\lambda}{2}\left(C_1^2 + C_2^2\right) \tag{52}$$

After substitution of (52) into (50),

$$\dot{T}_{D_{ave}} = -\lambda^2\left(mr_1\Gamma\right)^2\omega^2(\lambda+\Omega)k/2D_1 \tag{53}$$

Similarly for the rotor, the average energy dissipation rate is the sum of the two components of average dissipation rates.

$$\dot{T}_{R_{ave}} = \dot{T}_{R_{z_{ave}}} + \dot{T}_{R_{x_{ave}}} \tag{54}$$

where

$$\dot{T}_{R_{z_{ave}}} = -k_R \dot{\alpha}^2_{z_{ave}}$$

$$\dot{T}_{R_{x_{ave}}} = -k_R \dot{\alpha}^2_{x_{ave}}$$

Following the same procedure as above, it can be shown that,

$$\dot{\alpha}^2_{z_{ss_{ave}}} + \dot{\alpha}^2_{x_{ss_{ave}}} = (s-\lambda)^2 \left(C_3^2 + C_4^2\right) \tag{55}$$

and, therefore,

$$\dot{T}_{R_{ave}} = -(s-\lambda)^2 I_{R_1}^2 \omega^2 (\lambda - \Omega - 2s)^2 k_R / D_2 \tag{56}$$

By comparison of Equations (49), (53), and (56), it can be seen that $\dot{\gamma}$ can be written in terms of $\dot{T}_{R_{ave}}$ and $\dot{T}_{D_{ave}}$, as follows:

$$\dot{\gamma} = \frac{1}{H \sin\gamma} \left[\frac{\dot{T}_{D_{ave}}}{\lambda} + \frac{\dot{T}_{R_{ave}}}{\lambda - s} \right] \tag{57}$$

or

$$\frac{d}{dt} (H \cos\gamma)_{ave} = \dot{H}_{2_{ave}} = \frac{\dot{T}_{D_{ave}}}{\lambda} + \frac{\dot{T}_{R_{ave}}}{\lambda - s} \tag{58}$$

The terms within the bracket of Equation (57) are identical in form to those appearing in Likins' energy sink analysis.[8] As Likins indicates the terms $\dot{T}_{D_{ave}}/\lambda$ and $\dot{T}_{R_{ave}}/(\lambda - s)$ are the "first approximation" dissipative torques about the spin axis of the main body and spin axis of the rotor respectively, which is apparent from consideration of Equation (58). The implication here is that if the averaging technique of Flatley[7] were carried to a higher order, (e.g. first order approximation for main satellite angular rates, and second order approximations for damper and wheel deflections), additional terms may result in $F(\gamma)$, yielding additional, more complete stability information.

III. NUMERICAL RESULTS

A. Calculation of Stability Criteria for SAS-A

For stability, from consideration of $f'(\gamma_0) < 0$, at $\gamma_0 = 0°$ it is necessary that $F(0) < 0$. $F(0)$ was numerically evaluated using representative SAS-A parameters as listed below:

$A = 27.0$ kg-m^2	$k = 7.0 \times 10^{-5}$ nt-m-sec/rad.
$B = 28.54$ kg-m^2	$K = 6.10 \times 10^{-5}$ nt-m/rad.
$\Gamma = 0.44$ m.	$\Omega = 8.72 \times 10^{-3}$ rad/sec.
$r_0 = 0.019$ m.	$m = 0.2158$ kg.
$r_1 = 0.1833$ m.	$^*K_R = 71.6107$ nt-m/rad.
$I_{R_2} = 0.011519$ kg-m^2	$^*k_R = 0.006778$ nt-m-sec/rad.
$I_{R_1} = 0.0057595$ kg-m^2	

Four different values of s were considered: 0, 0.1 nominal, 0.5 nominal and the nominal value of 209.4 rad/sec.

We write $F(\gamma)$ as

$$F(\gamma) = \frac{H}{2A^2}\left[Q_1 + Q_2\right] \tag{58}$$

*Determined experimentally at The Applied Physics Laboratory, Johns Hopkins University.

where

$$Q_1 = -\left[(mr_1\,\Gamma)^2\,(\Omega+\lambda)^2\,k\lambda\right]\Big/D_1$$

and

$$Q_2 = \left[2\,I_{R_1}^2\,(2s-\lambda+\Omega)^2\,k_R\,(s-\lambda)\right]\Big/D_2$$

The results are summarized in the following table.

$s/\Omega_0 = q'$	$Q_1(0)$	$Q_2(0)$	$\left[2A^2/H\right]\cdot F(0)$
0	-2.448×10^{-7}	-2.949×10^{-18}	-2.448×10^{-7}
2401.3	-1.8379×10^{-5}	3.2185×10^{-6}	-1.516×10^{-6}
12,006.88	-1.3167×10^{-3}	4.015×10^{-4}	-0.9152×10^{-3}
24,013.7615	-0.4092	3.195×10^{-3}	-0.406

The system is stable for all four values of q', but the margin of stability for the two intermediate values of q' is not as great as at the nominal operating condition where the stability is insured by a factor of 128. This calculation does not guarantee the system stability during the actual spin-up process, but does give an indication of stability if, for some reason, the wheel does not reach its nominal operating angular velocity, s. (To study the problem of stability during spin-up, an equation for the motor torque would have to be included in the formulation with s now treated as a function of time instead of as a constant.) The sign of $Q_2(0)$, in the numerical example, verifies that only at very low values of q', is the effect of wheel damping stabilizing. The "X" appearing on the stability charts, Figures 4 and 6, refers to the SAS-A satellite under nominal operating conditions.

B. Calculation of s_{crit}

Using the SAS-A parameters listed in III.A., the critical value of wheel spin was calculated from Equation (47) to be $s_{crit} = 26.35$ rad/sec. Since the nominal value for s under normal SAS-A operating conditions is 209.4 rad/sec, $s > s_{crit}$.,

and the nutation angle of 180° (satellite inverted) becomes a point of unstable equilibrium, if the effects of wheel damping are neglected. This means that should SAS-A reach an inverted position, given a small perturbation, it would tend to restore itself to the "upright" position. (In this argument the effect of such discontinuities as nutation damper stops have not been included, but could be determined using a digital computer simulation of the nonlinear equations of motion with a suitable model for the stops.)

C. Calculation of Time Constant Associated With Nutation Angle Decay for $\gamma_0 = 0°$

The time constant associated with nutation angle decay is given by the reciprocal of the slope of $f(\gamma)$ at the equilibrium point. Equation (42) has the form $\dot{\gamma} = f(\gamma)$ and at an initial point of equilibrium, γ_0, $f(\gamma_0) = 0$. If we let $\gamma = \gamma_0 + x$ where x is small when compared with γ_0, then, $\dot{\gamma} = \dot{x}$, and $f(\gamma) \approx f(\gamma_0) + xf'(\gamma_0)$.

Thus, $\dot{x} \approx xf'(\gamma_0)$ and $dx/x = f'(\gamma_0)\,dt$. This differential equation has the exponential solution of the form: $x = x(0)\, e^{f'(\gamma_0)t} = x(0)\, e^{t/\tau}$ where τ is the exponential time constant, and $\tau = -1/f'(\gamma_0)$.

For SAS-A we are interested in the time constant associated with nutation angle decay for an initial equilibrium nutation angle of zero degrees. At $\gamma_0 = 0$, $f'(0) = F(0)$, and $\tau = -1/F(0)$. Using SAS-A parameters it was found that $\tau = 22.3$ minutes, which compares favorably with previous numerical integration results not including wheel damping.[1]

IV. CONCLUDING REMARKS

As a result of the present stability analysis and numerical results the following conclusions can be made:

1. The stability criteria obtained for this system by means of averaging[7] the "first order" perturbations on the system nutation angle can be reduced to the criteria emanating from Likins' energy sink analysis. The implication is that higher order terms would have to be also included in the averaging process to yield more complete stability information.

2. In the absence of wheel damping, some (but not all) of the previously derived[1] Routh-Hurwitz necessary and sufficient conditions can be obtained from the present analysis.

3. In the absence of wheel damping, the nominal SAS-A rotor spin rate is such that a nutation angle of 180 degrees (inversion) is a position of unstable equilibrium.

4. A numerical evaluation of the analytical stability criterion developed here, using SAS-A satellite parameters and measured wheel damping data, indicates that system stability is insured by a factor of 128 under the normal operating conditions. The system is also stable at smaller values of rotor spin rate, although the margin of stability is somewhat reduced.

5. The time constant associated with nutation angle decay under the normal SAS-A operating conditions is 22.3 minutes, and is not appreciably degraded by the measured energy dissipation in the wheel.

The nonlinear equations of motion derived here will be solved by numerical integration techniques in order to 1) verify the results of the present analytical study, 2) consider further stability problems during momentum wheel spin-up, and 3) evaluate the effects of external perturbations (such as aerodynamic and gravity gradient torques) on the results reported here. The results of these numerical studies will be reported subsequently.

REFERENCES

1. Bainum, P. M., Fuechsel, P. G., and Mackison, D. L., "Motion and Stability of a Dual-Spin Satellite with Nutation Damping," Journal of Spacecraft and Rockets, Vol. 7, No. 6, June 1970, pp. 690-696; also as TG-1072, June 1969, Applied Physics Laboratory, The Johns Hopkins University, Silver Spring, Md.

2. Mingori, D. L., "Effects of Energy Dissipation on the Attitude Stability of Dual-Spin Satellites," AIAA Journal, Vol. 7, No. 1, January 1969, pp. 20-27.

3. Sen, A. K., and Fleisher, G., "On the Attitude Stability of the SAS-A Spacecraft," Branch Report No. 204 (Revised), Feb. 18, 1970, Stabilization and Control Branch, NASA Goddard Space Flight Center, Greenbelt, Maryland.

4. Tossman, B. E., "Variable Parameter Nutation Damper for SAS-A," AIAA Paper No. 70-972, AIAA Guidance, Control, and Flight Mechanics Conference, Santa Barbara, Calif., August 1970.

5. Likins, Peter W., Tseng, Gan-Tai, and Mingori, D. L., "Stable Limit Cycles Due to Nonlinear Damping in Dual-Spin Spacecraft," AIAA Paper No. 70-1044, AAS/AIAA Astrodynamics Conference, Santa Barbara, Calif., August 1970.

6. Whittaker, E. T., A Treatise on the Analytical Dynamics of Particles and Rigid Bodies, 4th ed., Cambridge University Press. Cambridge, England, 1959, pp. 41-44.

7. Flatley, T. W., "Equilibrium States for a Class of Dual-Spin Spacecraft," Ph.D. dissertation, The Catholic University of America, School of Engineering and Architecture, Washington, D. C., 1970.

8. Likins, Peter W., "Attitude Stability Criteria for Dual-Spin Spacecraft," Journal of Spacecraft and Rockets, Vol. 4, No. 12, December 1967, pp. 1638-1643.

APPENDIX A

The following two figures show the results of wheel damping tests performed at the Applied Physics Laboratory by Mr. R. E. Fischell and Mr. W. Radford. The values of K_R and k_R were determined for both air and vacuum conditions. With the wheel initially stationary (Figure A.1) and then initially spinning (Figure A.2) and with the wheel symmetry axis vertical, an initial impulse was applied to the outer rim of the wheel. Instrumentation recorded the vertical displacement of the wheel as a function of time. It can be seen that the transient responses shown in the Figures are, for all practical purposes, characteristic of a second order linear system. Values of K_R and k_R selected for numerical examples in this paper represent the most pessimistic case (worst destabilizing effect).

The wheel deflection Equations (21) and (22) are of the form:

$$I_{R_1} \ddot{\alpha} + k_R \dot{\alpha} + \left[K_R + I_{R_1} \left(\omega_2 + s\right)^2\right] \alpha = f(t) \qquad \text{(A1)}$$

which have a transient solution,

$$\alpha = \alpha_0 e^{-\left(k_R/2 I_R\right) t} \left[\sin\left(\Omega_R t + \psi_0\right)\right] \qquad \text{(A2)}$$

where α_0 and ψ_0 are determined from the boundary conditions. The time constant, τ, is the value of t when $k_R\, t/2I_R = 1$. Thus

$$k_R = 2I_R/\tau \qquad \text{(A3)}$$

The damped natural frequency, Ω_R, is related to the system parameters according to:

$$\Omega_R = \frac{1}{2}\left|\left(\frac{k_R}{I_{R_1}}\right)^2 - 4\left[\frac{K_R + I_{R_1}\left(\omega_2 + s\right)^2}{I_{R_1}}\right]\right|^{1/2} \qquad \text{(A4)}$$

and $\left(K_R/I_{R_1}\right)^{1/2}$ is the undamped natural frequency.

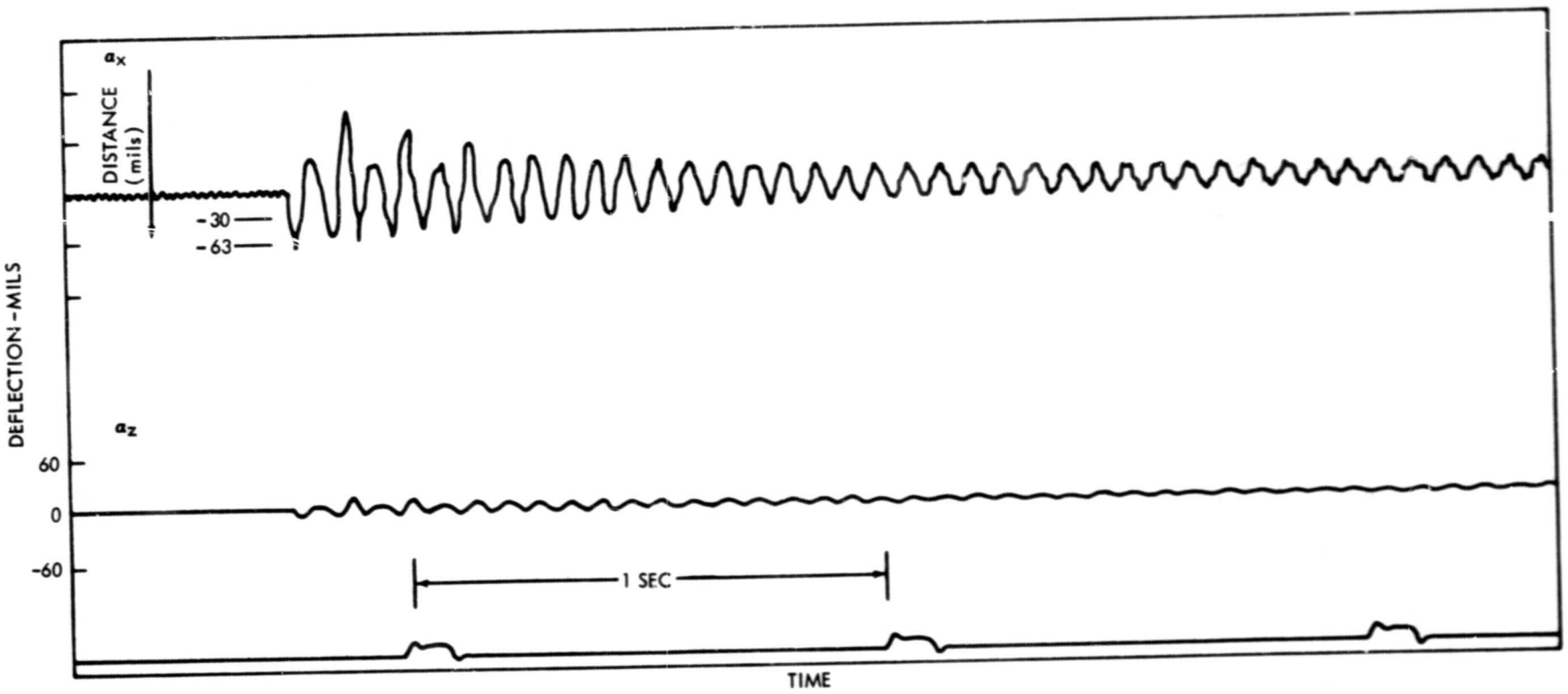

Figure A-1. SAS-A Wheel Damping Test-Wheel Initially Stationary

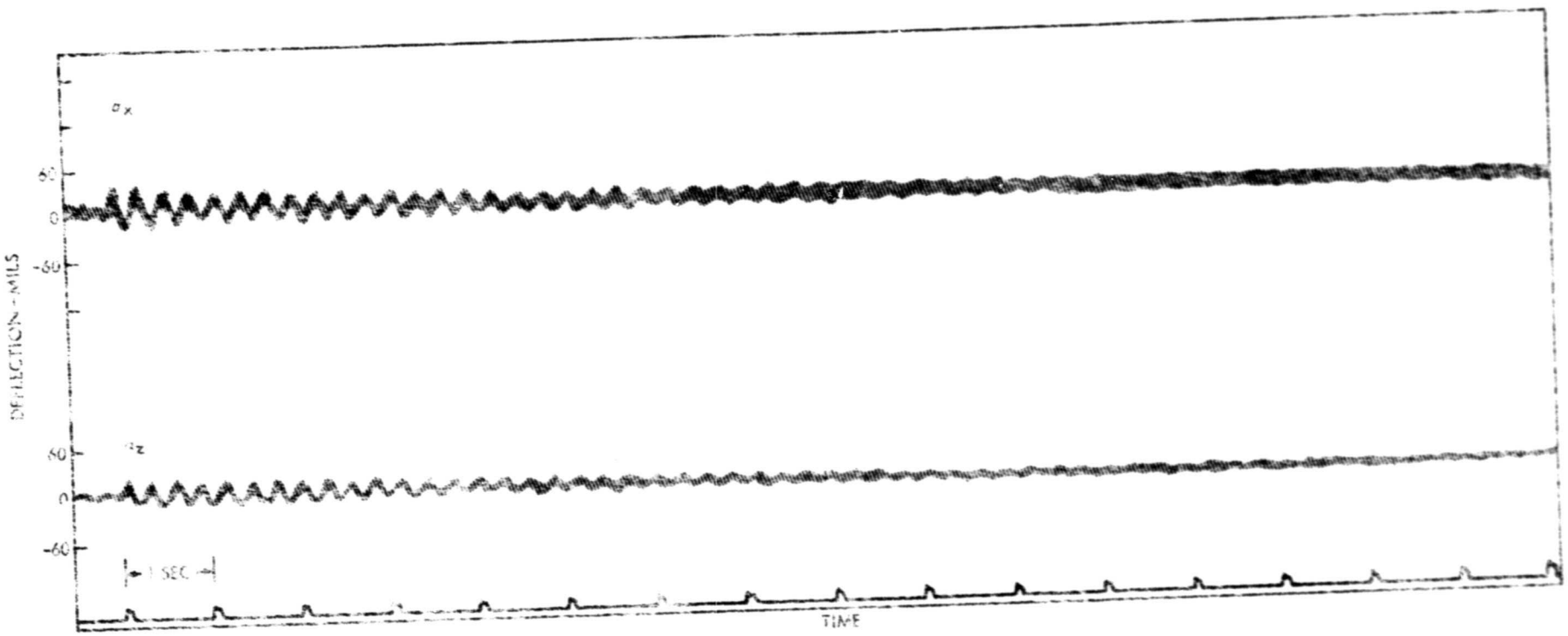

Figure A-2. SAS-A Wheel Damping Test-Wheel Rotating